

## Universal dynamics of spatiotemporal entrainment with phase symmetry

Jorge Palacio Mizrahi, Danny Zilberg, and Omri Gat 

*The Racah Institute of Physics, The Hebrew University of Jerusalem, Jerusalem 9190401, Israel*

 (Received 23 July 2021; accepted 16 June 2023; published 20 July 2023)

We study the entrainment of a localized pattern to an external signal via its coupling to zero modes associated with broken symmetries. We show that when the pattern breaks internal symmetries, entrainment is governed by a multiple degrees-of-freedom dynamical system that has a universal structure, defined by the symmetry group and its breaking. We derive explicitly the universal locking dynamics for entrainment of patterns breaking internal phase symmetry, and calculate the locking domains and the stability and bifurcations of entrainment of complex Ginzburg-Landau solitons by an external pulse.

DOI: [10.1103/PhysRevE.108.014120](https://doi.org/10.1103/PhysRevE.108.014120)

### I. INTRODUCTION

Entrainment is a central paradigm of nonlinear science, which can arise whenever a continuous symmetry is broken in two or more coupled systems. When the broken symmetry is time-translation invariance, entrainment leads to *synchronization*, of which the simplest example is the frequency locking of limit cycles of nonlinear oscillators, either by external injection, as in the van der Pol circuit [1], or by mutual interaction, such as in Huygens' pendulum clocks [2]; mutual synchronization can give rise to collective behavior when the number of synchronized oscillators is large [3–5]. Synchronization occurs on more complex attractors as well, including quasiperiodic [6] and chaotic [7–10] attractors. Synchronization may take place in spatially extended systems [11,12], of which recently studied examples include dissipative optical soliton breathers [13], Kerr [14,15] and laser [16] frequency combs, and optomechanical [17,18] oscillators.

Entrainment of steady states breaking *space*-translation invariance leads to wave-number locking, either by external injection [19–22], or by mutual interaction [23,24]. Patterns breaking both time- and space-translation invariance can be spatiotemporally entrained by spatially uniform temporally periodic driving [25–27], as well as by injection of traveling waves [28–33].

The entrainment phenomenon is ubiquitous because it is tied to spontaneous symmetry breaking. The entrainment dynamics is *universal* for the same reason. For example, synchronization of a limit cycle always involves the locking dynamics of a phase, which is the variable associated with the zero mode that appears in the stability spectrum of the limit cycle as a result of the breaking of a continuous time-translation invariance to a discrete one; this mechanism is independent of the details of the dynamical system, and for this reason the phase evolution is captured by the universal Adler equation [2].

Here, we study the entrainment effect for localized patterns that break *internal symmetries* in addition to space-translation

invariance. Then, the stability spectrum of the pattern has internal-symmetry zero modes in addition to the translation zero mode. A general perturbation couples to all the zero modes, producing a multiple degrees-of-freedom locking dynamical system that nevertheless has a universal structure for each set of broken internal symmetries.

We present two sets of results: We first derive the universal form of the locking dynamical system governing the entrainment of localized patterns with an internal phase symmetry, for which there are two symmetry generators, one for translations and one for phase shifts. It follows that entrainment in this class is governed by a two-degrees-of-freedom dynamical system, which depends on two disparity parameters—relative velocity and frequency detuning. We show that for a given external injection there is a bounded locking domain in the space of possible disparities where the pattern can be stably entrained, and that the locking domain depends linearly on the strength of the coupling.

Our second set of results is derived for a concrete example of pulse solutions of the cubic-quintic complex Ginzburg-Landau (QCGL) equation injected with Gaussian pulses. We present locking diagrams showing the locking domains for several parameter choices of the QCGL equation and injected pulses. The diagrams exhibit the full complexity of a two-parameter family of two-degrees-of-freedom dynamical systems, including multistability and curves of saddle-node and Hopf bifurcations, tangent at Bogdanov-Takens bifurcation points.

### II. LOCKING DYNAMICS WITH AN INTERNAL PHASE SYMMETRY

Consider a pattern-forming dynamical system in one space dimension

$$\frac{\partial \Psi_u}{\partial t} = \mathcal{N}[\Psi_u], \quad (1)$$

for the multicomponent field  $\Psi_u(x)$ . The nonlinear operator  $\mathcal{N}$  respects space-translation symmetry,

$$\mathcal{N}[\Psi(\cdot - \xi)](x) = \mathcal{N}[\Psi(\cdot)](x - \xi), \quad (2)$$

\*omrigat@mail.huji.ac.il

for any shift  $\xi$ , and an internal symmetry

$$\mathcal{N}[G\Psi] = G\mathcal{N}[\Psi] \quad (3)$$

for a continuous (Lie) group of global operations  $G$  (group action) that mix the components of  $\Psi$  but do not affect the spatial coordinate  $x$ .

We assume that Eq. (1) has at least one stable spatially uniform, internal-symmetry invariant time-independent solution, and a stable pattern solution,  $\Psi_0(x)$ , that is localized near  $x = 0$ , and tends to uniform solutions as  $x \rightarrow \pm\infty$ . In the frame where  $\Psi_0(x)$  is stationary,  $\mathcal{N}[\Psi_0] = 0$ .  $\Psi_0$  breaks translation symmetry by being localized, and we assume that it is not invariant under all the group operations, so that it breaks internal symmetry as well.

We next let the pattern  $\Psi_0$  interact with a weak external signal  $F$  that is localized near  $x = 0$  at  $t = 0$ , moving with a constant velocity  $v$ , and undergoing internal symmetry transformations at a constant rate relative to the free pattern, so that the equation of motion for the perturbed field  $\Psi$  becomes

$$\frac{\partial\Psi}{\partial t} = \mathcal{N}[\Psi] + e^{-iGt}F(x - vt); \quad (4)$$

here, the operation  $\mathcal{G}$  is an element of the Lie algebra action on the internal space of  $\Psi$ , induced by the group action of (3), and  $e^{-iGt}$  is a one-parameter subgroup of operations.

When  $t < 0$  and  $|vt|$  is large, the only effect of the external injection is a slight perturbation in the tail of the pattern  $\Psi_0$ , so that

$$\Psi(x, t) \underset{t \rightarrow -\infty}{\sim} \Psi_0(x). \quad (5)$$

However, when  $t$  approaches zero, the injected signal overlaps with the nontrivial region of the localized pattern, and its interaction with the position and the internal symmetry of the pattern may lead to two distinct outcomes as  $t \rightarrow +\infty$ . If the interaction is weak, then the injected signal eventually overtakes the localized pattern with the interaction becoming negligible again when  $|vt|$  is large, so that the net asymptotic result of the interaction is a displacement  $x_\infty$  and an internal symmetry transformation  $G_\infty$  of the pattern:

$$\text{Unlocked: } \Psi(x, t) \underset{t \rightarrow \infty}{\sim} G_\infty \Psi_0(x - x_\infty). \quad (6)$$

On the other hand, if the interaction is strong enough and effective, then the pattern becomes entrained: That is, as  $t \rightarrow \infty$  it may become stationary in the *injection* frame, so that the pattern-signal interaction remains strong enough to maintain locking indefinitely with displacement  $y_\infty$  and internal symmetry transformation  $\Gamma_\infty$  relative to the entraining signal,

$$\text{Locked: } \Psi(x, t) \underset{t \rightarrow \infty}{\sim} \Gamma_\infty e^{-iGt} \Psi_0(x - vt - y_\infty). \quad (7)$$

Our goal is to determine which combinations of injection parameters,  $F$ ,  $v$ ,  $\mathcal{G}$ , lead to asymptotic entrainment as in (7). The problem is difficult to solve in general, and moreover, our results below suggest that there exist nonstationary entrained states. In this view, we focus in the following on the special case of a pattern breaking an internal phase symmetry. Then  $\Psi = (\psi, \psi^*)$ ,  $\psi$  a complex-valued function, and  $\mathcal{N}[\Psi] = (\mathcal{O}[\Psi], \mathcal{O}[\Psi]^*)$ , where  $\mathcal{O}$  is a complex-function-valued differential operator, and  $*$  complex conjugation. The symmetry operation is  $G_\varphi \Psi = (e^{i\varphi}\psi, e^{-i\varphi}\psi^*)$ , and the injection takes

the form  $e^{-iGt}F = (f e^{-i\omega t}, f^* e^{i\omega t})$ , where  $f$  is a complex-valued function localized near  $x = 0$ , and  $\omega$  is the relative injection-pattern frequency.

The variables associated with the broken translation and phase symmetries are the position  $\xi$  and overall phase  $\varphi$  of the localized pattern  $\psi_0$ . Our next goal is to derive the locking dynamical system for  $\xi$  and  $\varphi$ . For this purpose note that even though  $f$  is assumed small,  $\xi$  and  $\varphi$  may become large for  $t \gg 1$ , since they are associated with broken symmetries, and therefore experience no restoring force. We accordingly assume that

$$\psi(x, t) = \{\psi_0[x - \xi(t)] + \psi_1[x - \xi(t), t]\}e^{-i\varphi(t)}, \quad (8)$$

where  $\psi_1$  is a small shape perturbation.

Using this ansatz in Eq. (4) gives

$$\frac{\partial\Psi_1}{\partial t} + \frac{d\xi}{dt}\Psi_\xi + \frac{d\varphi}{dt}\Psi_\varphi = \mathcal{L}\Psi_1 + F, \quad (9)$$

where  $\mathcal{L}$  is the linear stability operator of the pattern, i.e., the functional derivative of  $\mathcal{N}$  with respect to  $\Psi$ , evaluated at  $\Psi_0$ , and  $\Psi_\xi = -[\psi'_0, (\psi'_0)^*]$ ,  $\Psi_\varphi = (-i\psi_0, i\psi_0^*)$ , are the zero modes associated with the broken translation and phase symmetries (respectively),  $\mathcal{L}\Psi_\xi = \mathcal{L}\Psi_\varphi = 0$ . The assumption that  $\Psi_0$  is a stable pattern implies that the rest of the spectrum of  $\mathcal{L}$  is in the left half of the complex plane. We make the stronger assumption that the spectrum of  $\mathcal{L}$ , other than the two symmetry-related zero eigenvalues, is separated from the imaginary axis by a gap, guaranteeing that  $\Psi_1$  remains small for a sufficiently small injection.

The equations of motion for  $\xi$  and  $\varphi$  should be derived from (9); however, these variables are not fully defined by (8), because a small change in  $\xi$  and  $\varphi$  can be absorbed into  $\psi_1$ . This ambiguity is removed by requiring that

$$\langle \bar{\Psi}_\xi, \Psi_1 \rangle = \langle \bar{\Psi}_\varphi, \Psi_1 \rangle = 0, \quad (10)$$

where  $\bar{\Psi}_\xi = (\bar{\psi}_\xi, \bar{\psi}_\xi^*)$  and  $\bar{\Psi}_\varphi = (\bar{\psi}_\varphi, \bar{\psi}_\varphi^*)$  are the zero eigenfunctions of  $\mathcal{L}^\dagger$  (the adjoint of  $\mathcal{L}$ ) corresponding to  $\Psi_\xi$  and  $\Psi_\varphi$ , normalized with  $\langle \bar{\Psi}_\xi, \Psi_\xi \rangle = \langle \bar{\Psi}_\varphi, \Psi_\varphi \rangle = 1$ ; we use the inner product

$$\langle \Phi, \Psi \rangle \equiv \langle (\phi, \tilde{\phi}), (\psi, \tilde{\psi}) \rangle = \frac{1}{2} \int_{-\infty}^{\infty} dx (\phi^* \psi + \tilde{\phi}^* \tilde{\psi}). \quad (11)$$

Projecting Eq. (9) on  $\bar{\Psi}_\xi$  and  $\bar{\Psi}_\varphi$  now gives

$$\frac{d\xi}{dt} = \langle \bar{\Psi}_\xi, F \rangle \equiv c_\xi(\xi - vt, \varphi - \omega t), \quad (12)$$

$$\frac{d\varphi}{dt} = \langle \bar{\Psi}_\varphi, F \rangle \equiv c_\varphi(\xi - vt, \varphi - \omega t), \quad (13)$$

and making a change of variables to the position and phase shifts,  $y = \xi - vt$  and  $\theta = \varphi - \omega t$  (respectively), we finally obtain

$$\frac{dy}{dt} = c_\xi(y, \theta) - v, \quad (14)$$

$$\frac{d\theta}{dt} = c_\varphi(y, \theta) - \omega, \quad (15)$$

where the real-valued locking functions  $c_\xi$  and  $c_\varphi$  are localized in  $y$  and periodic in  $\theta$ . Equations (14) and (15) comprise the universal locking dynamical system for localized patterns

with an internal phase symmetry interacting with an external signal. The (stable) fixed points of the locking system correspond to (stable) entrained steady states of the pattern. The examples studied below show that the structure and properties of the stable entrained states can be quite varied and complex. Nevertheless, some general features follow directly from the equations.

First note that the locking functions take the forms

$$c_\xi(y, \theta) = \mathcal{I}_\xi \equiv g(y) \cos[\theta - \alpha(y)], \quad (16)$$

$$c_\phi(y, \theta) = \mathcal{I}_\phi \equiv h(y) \cos[\theta - \beta(y)], \quad (17)$$

where

$$\mathcal{I}_{\xi,\phi} = \text{Re} \left( e^{i\theta} \int_{-\infty}^{\infty} \bar{\psi}_{\xi,\phi}(x) f(x-y) dx \right). \quad (18)$$

Entrained steady states are solutions  $(\hat{y}, \hat{\theta})$  of the system

$$h(\hat{y}) \cos[\hat{\theta} - \alpha(\hat{y})] = v, \quad g(\hat{y}) \cos[\hat{\theta} - \beta(\hat{y})] = \omega; \quad (19)$$

eliminating  $\hat{\theta}$  gives the equation

$$v = (h/g)(\omega \cos \gamma \pm \sin \gamma \sqrt{g^2 - \omega^2}), \quad (20)$$

where  $\gamma = \beta - \alpha$ , and all functions are evaluated at  $\hat{y}$ .

Disparity parameters combinations  $(\omega, v)$  for which (20) has one or more solutions belong to the *locking domain*, where entrainment is possible for a given injection signal  $f$ . Since  $f$ ,  $\bar{\psi}_\xi$ , and  $\bar{\psi}_\phi$  are localized, it follows that the locking functions  $g, h \rightarrow 0$  for  $|y| \rightarrow \infty$ , and are therefore bounded, so that the locking domain is bounded in the rectangle  $|v| < \max(|h|)$ ,  $|\omega| < \max(|g|)$ . For any  $\omega$  in the latter interval, (20) defines a function  $v_\omega(y)$  defined for all  $y$  such that  $g^2(y) > \omega^2$ , whose range is a collection of one or more intervals, and the locking domain can be pieced together from these intervals by running over the allowed values of  $\omega$ ; several examples are shown below.

The *stable* locking domain consists of those disparity combinations  $(\omega, v)$  in the locking domain for which the eigenvalues of the Jacobian matrix

$$J = \begin{pmatrix} \partial_y c_\xi & \partial_\theta c_\xi \\ \partial_y c_\phi & \partial_\theta c_\phi \end{pmatrix} \quad (21)$$

have negative real parts for at least one entrained steady state. For such entrained states  $\text{tr} J < 0$  and  $\det J > 0$ , and therefore at the boundary of the stable locking region either  $\text{tr} J = 0$  or  $\det J = 0$ . The latter equality, together with the fixed-point condition (19), implicitly defines a curve or curves of saddle-node bifurcations on the stability boundary, and the former defines a curve or curves of Hopf bifurcations; the curves of both kinds meet at points of Bogdanov-Takens bifurcations where both eigenvalues are zero [34]. Note that the locking functions  $g$  and  $h$ , as well as the Jacobian matrix  $J$  depend linearly on  $f$ , so that the locking domains and stable locking domains scale linearly with the injection amplitude.

### III. ENTRAINMENT OF COMPLEX GINZBURG-LANDAU PULSES

The cubic-quintic complex Ginzburg-Landau (QCGL) equation, defined by the nonlinear operator

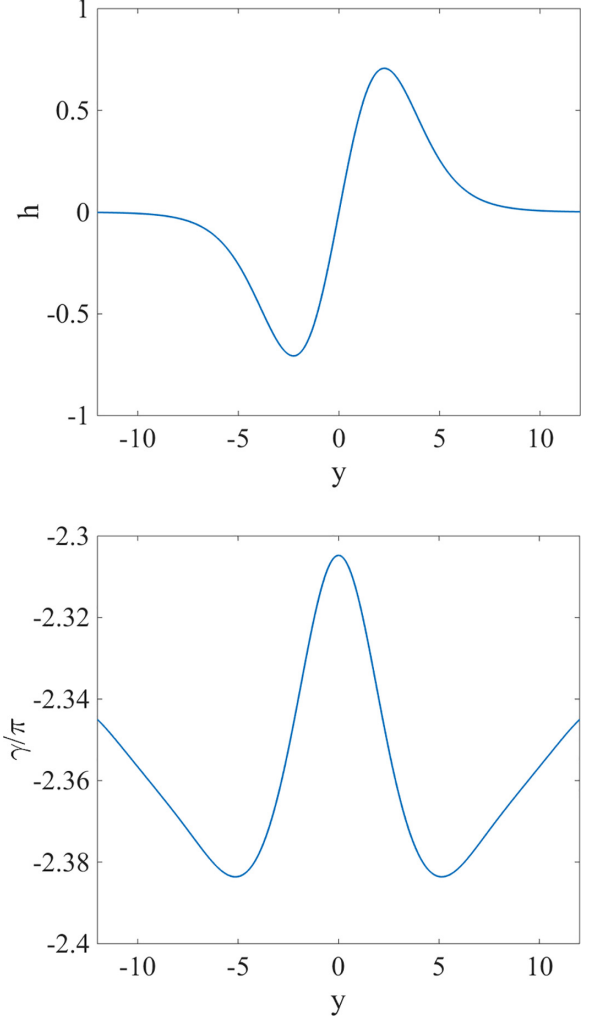


FIG. 1. The locking functions  $h$  (top) and  $\gamma$  (bottom), for entrainment of a QCGL by an externally injected Gaussian pulse. The QCGL parameters are  $\beta = 0.8$ ,  $\delta = -0.1$ ,  $\epsilon = 0.8$ ,  $\mu = -0.5$ ,  $\nu = -0.1$ . [See Eq. (22) for the parameter definitions.] Gaussian injection parameters are  $a = 0.1$  (here and below) and  $c = 0.2$  (top),  $c = 1.3$  (bottom).

$$\begin{aligned} \mathcal{O}[\Psi] = & (\delta - i\omega_0)\psi + (\beta + i/2)\partial^2\psi/\partial x^2 \\ & + (\epsilon + i)|\psi|^2\psi + (\mu + i\nu)|\psi|^4\psi, \end{aligned} \quad (22)$$

with real parameters  $\delta, \beta, \epsilon, \mu < 0$ , and  $\nu$ , has an internal phase symmetry, and is known to have stable pulse solutions in some parameter ranges [35], which become stationary for appropriately chosen  $\omega_0$ . We will consider entrainment of QCGL pulses by a Gaussian pulse  $f(x) = ae^{-cx^2}$ ,  $a, c > 0$ . Owing to the parity symmetry of the QCGL equation, its pulse solutions are even,  $\psi_0(-x) = \psi_0(x)$ , making  $h$  an odd function and  $g, \alpha$ , and  $\beta$  even functions of  $y$ . These symmetries imply that if  $(\hat{y}, \hat{\theta})$  is a fixed point of (14) and (15) with detuning parameters  $v, \omega$ , then so are  $(-\hat{y}, \hat{\theta})$  with  $-v, \omega$ , and  $(-\hat{y}, \hat{\theta} + \pi)$  with  $v, -\omega$ , and therefore the locking domain is symmetric with respect to sign flips of both  $v$  and  $\omega$ .

Furthermore, it follows from (21) that under a sign flip of  $\hat{y}$  the (off-)diagonal elements of  $J$  remain invariant (change sign), so that  $\text{tr} J$  and  $\det J$  are unchanged, while a  $\pi$  shift of  $\hat{\theta}$

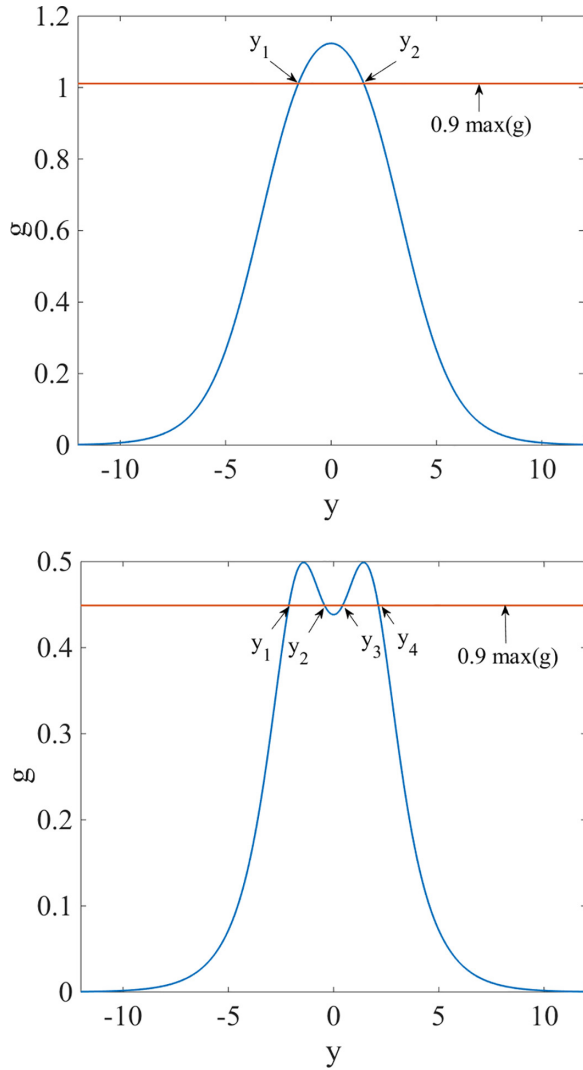


FIG. 2. The locking function  $g$  for entrainment of a QCGL pulse by an externally injected Gaussian pulse. The  $g$  values marked by the horizontal lines represent admissible values of frequency disparity  $\omega$ , and the displacement values  $y$  for which  $g^2(y) > \omega^2$  are those for which there are entrained steady states for this value of  $\omega$ . When the injected signal is broad (top),  $g$  is unimodal, and there is a single interval of locked states for each  $\omega$ , and when the injected signal is narrow (right),  $g$  is bimodal, and there are two disjoint intervals of locked states for sufficiently large  $\omega$ . The QCGL and parameters are as in Fig. 1; the injection width parameters are  $c = 0.2$  (top) and  $c = 1.3$  (bottom).

makes all the elements of  $J$  flip sign. Consequently, the *stable* locking domain is invariant under a sign flip of  $v$ , while at most one of the locking states related by a sign change of  $\omega$  can be stable.

Figures 1 and 2 present numerical examples of the locking functions. As shown in Fig. 2, the even function  $g$  can be either unimodal with a maximum at  $y = 0$ , or bimodal, with a minimum at  $y = 0$ . In the former case, there is a single interval of velocity locking intervals  $v$  for each admissible  $\omega$  and sign choice in (20); in the latter case, there are two locking intervals for each  $\omega$  larger than the local minimum of  $g$  at  $y = 0$ . Consequently, the locking domains for broad

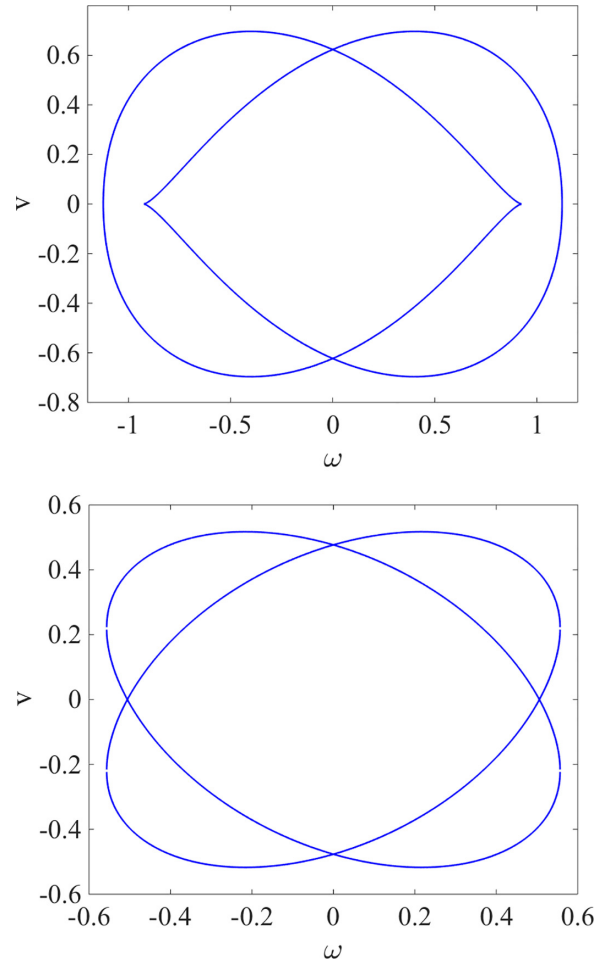


FIG. 3. Locking diagrams showing boundaries of branches of steady states of QCGL pulses entrained by an externally injected Gaussian pulse, with signal-pulse displacements  $\hat{y}$  and phase shifts  $\hat{\phi}$  depending smoothly on the frequency disparity  $\omega$  and velocity disparity  $v$ . QCGL and injection parameters are as in the top and bottom panels of Fig. 1 (respectively).

and narrow injections are qualitatively different, as shown below. Unlike  $g$ , the locking functions  $h$  and  $\gamma$  have the same qualitative structure for all QCGL and injection parameters that we tested; examples are shown in Fig. 1.

Figure 3 shows two examples of locking domains of the same QCGL pulse entrained by injected Gaussians of different widths. The solid curves are boundaries of branches of entrained steady states that are solutions of (19); the boundary curves consist of saddle-node bifurcation points. In the top panel the injected pulse is wide, making the locking function  $g$  unimodal, with a single interval of solutions of (20) for each  $\omega$ , as in the example shown in the top panel of Fig. 2; it gives two overlapping teardrop-shaped locking branches that are individually invariant under  $v \leftrightarrow -v$ , and are mapped to each other by  $\omega \leftrightarrow -\omega$ . Of the two branches, exactly one, the *principal branch*, consists entirely of stable locked states, while the locked states of the secondary branch are all unstable. The similarly structured locking diagram in the top panel of Fig. 4 shows the boundary of the principal branch with a solid curve as in Fig. 3, and the boundary of the secondary branch

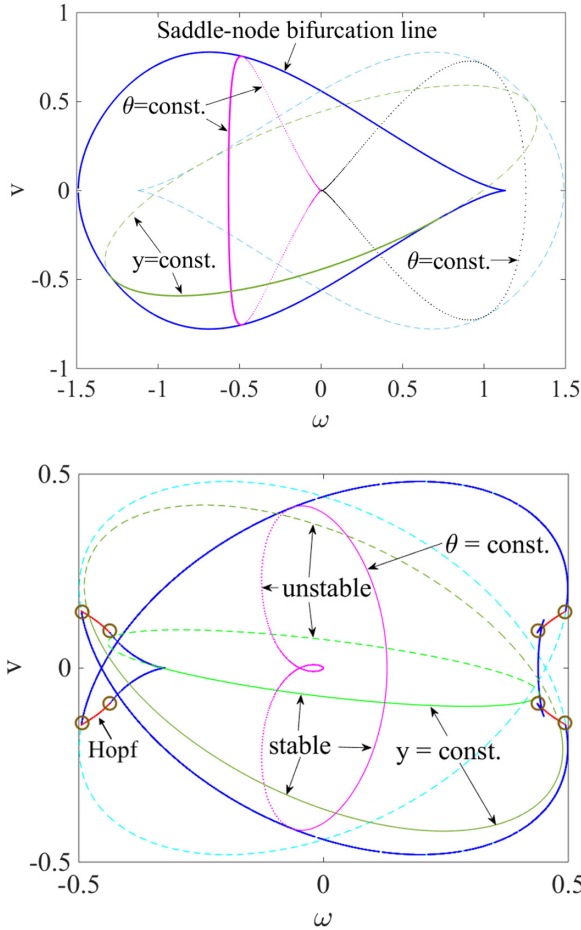


FIG. 4. Locking diagrams for QCGL and injection parameters  $\beta = 0.5$ ,  $\delta = -0.1$ ,  $\epsilon = 1.4$ ,  $\mu = -0.1$ ,  $\nu = 0.2$ ,  $c = 3$  (top), and  $\beta = 0.8$ ,  $\delta = -0.1$ ,  $\epsilon = 0.8$ ,  $\mu = -0.5$ ,  $\nu = -0.1$ ,  $c = 1.3$  (bottom). The boundaries of the stable part of the principal branch of entrained steady states (solid curves) consist of saddle-node bifurcations and Hopf bifurcations (in the bottom panel). The bifurcation curves of the two types meet at Bogdanov-Takens bifurcation points (circled). Unstable branch boundaries are shown with dashed curves. Interior curves show subbranches of entrained states with constant injection-pulse displacement  $\hat{y}$  or phase shift  $\hat{\theta}$ ; solid (dashed/dotted) parts of the curves show stable (unstable) parts, respectively of the subbranches.

is marked by a dashed curve. This figure also shows contours of constant- $\hat{y}$  and  $\hat{\theta}$  locked states, with solid (dashed) curves representing stable (unstable) solutions respectively. Note that Eqs. (19) imply that constant- $\hat{y}$  curves are ellipses or ellipse arcs. The top panel of Fig. 5 shows the locking diagram of Fig. 3 (top) with the principal branch coordinatized by  $\hat{y}$  and  $\hat{\theta}$ .

In contrast with these examples, the bottom panels of Figs. 3–5 show locking diagrams obtained with a bimodal locking function  $g$ , which produces two disjoint  $v$  locking intervals for large enough  $\omega$ . Consequently, the two ovals in the locking diagram shown in the bottom panel of Fig. 3 are boundaries of a *single* branch—the principal branch, that is invariant under sign changes of both  $v$  or  $\omega$ , and is double valued where the oval interiors overlap. However, in this case some of the principal branch locking states undergo Hopf bifurcations,

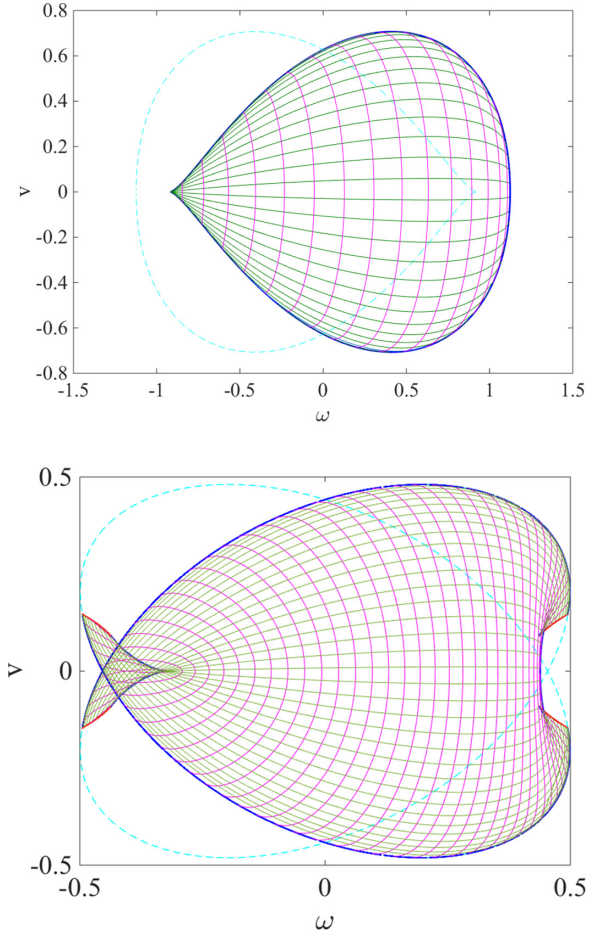


FIG. 5. Locking diagrams with QCGL and injection parameters as in the top and bottom panels of Fig. 1 (respectively). Branch and stability boundaries are marked as in Fig. 4. The stable parts of the principal branches are coordinatized by the curves of constant- $\hat{y}$  entrained states (horizontal) and constant- $\hat{\theta}$  states (vertical).

so only a part of the entrained steady states are stable. The Hopf bifurcation curves shown in the locking diagram of Fig. 4 (bottom), make up the boundary of the stable locking domain together with the saddle-node bifurcation curves. The two kinds of bifurcation curves meet at Bogdanov-Takens bifurcation points [34] that are circled in Fig. 4 (bottom). The locking diagram of Fig. 5 (bottom) shows this stable locking domain, coordinatized with constant- $\hat{y}$  and constant- $\hat{\theta}$  curves.

Finally, we note that since the locking domains scale linearly with the amplitude of injection, the locking diagrams of Figs. 3–5 can be viewed as two-dimensional sections of *cones* in a three-dimensional parameter space of  $\omega$ ,  $v$  and injection amplitude.

#### IV. CONCLUSIONS

Entrainment takes place when nonlinear systems with broken continuous symmetries interact. The fundamental property of entrainment phenomena is the sharp locking transition of the symmetry-breaking variables. The locking transition is a manifestation of a bifurcation in the locking dynamical system that governs the evolution of

the symmetry-breaking variables. In standard entrainment scenarios a single symmetry is broken—most notably time-translation invariance in synchronization. However, patterns in extended systems often break internal symmetries as well as space-translation invariance. Here, we have shown that when localized patterns with an internal symmetry are spatiotemporally forced, the locking dynamics becomes a multiple degrees-of-freedom system, whose form is universal within a symmetry class.

Focusing on the case of externally forced patterns with an internal phase symmetry, we demonstrated two-degrees-of-freedom locking effects, including entrainment bistability, Hopf, and Bogdanov-Takens bifurcations. Even though here we studied in detail only the stationary entrained states, our analysis makes it clear that much of the complexity of two-degrees-of-freedom dynamical systems can be realized in the

locking dynamics; for example, the occurrence of Hopf bifurcations implies that oscillatory “breather” entrainment can be realized on limit cycles of the locking system.

The shown examples of locking domains are two-dimensional sections of cones that are actually tips of three-dimensional Arnold tongues [36]. In single-variable locking Arnold tongues emerge at all commensurate frequencies, yielding locking diagrams with a fractal structure. We conjecture that beyond the fundamental entrainment that was studied here, entrainment of patterns with internal symmetries exhibits a complex structure of harmonic entrainment.

#### ACKNOWLEDGMENTS

This work was supported by the Israel Science Foundation under Grants No. 1428/15 and No. 2403/20.

- 
- [1] B. van der Pol, A theory of the amplitude of free and forced triode vibrations, *Radio Rev. (later Wireless World)* **1**, 701 (1920).
  - [2] A. Pikovsky, M. Rosenblum, and J. Kurths, *Synchronization* (Cambridge University Press, New York, 2001).
  - [3] Y. Kuramoto, Self-entrainment of a population of coupled nonlinear oscillators, in *International Symposium on Mathematical Problems in Theoretical Physics*, edited by H. Araki (Springer, Berlin, 1975), pp. 420–422.
  - [4] J. A. Acebrón, L. L. Bonilla, C. J. Pérez Vicente, F. Ritort, and R. Spigler, The Kuramoto model: A simple paradigm for synchronization phenomena, *Rev. Mod. Phys.* **77**, 137 (2005).
  - [5] A. Arenas, A. Díaz-Guilera, J. Kurths, Y. Moreno, and C. Zhou, Synchronization in complex networks, *Phys. Rep.* **469**, 93 (2008).
  - [6] V. Anishchenko, S. Nikolaev, and J. Kurths, Winding number locking on a two-dimensional torus: Synchronization of quasiperiodic motions, *Phys. Rev. E* **73**, 056202 (2006).
  - [7] L. M. Pecora and T. L. Carroll, Synchronization in Chaotic Systems, *Phys. Rev. Lett.* **64**, 821 (1990).
  - [8] U. Parlitz, L. Junge, W. Lauterborn, and L. Kocarev, Experimental observation of phase synchronization, *Phys. Rev. E* **54**, 2115 (1996).
  - [9] M. G. Rosenblum, A. S. Pikovsky, and J. Kurths, Phase Synchronization of Chaotic Oscillators, *Phys. Rev. Lett.* **76**, 1804 (1996).
  - [10] A. E. Hramov and A. A. Koronovskii, An approach to chaotic synchronization, *Chaos* **14**, 603 (2004).
  - [11] A. L. Lin, M. Bertram, K. Martinez, H. L. Swinney, A. Ardelea, and G. F. Carey, Resonant Phase Patterns in a Reaction-Diffusion System, *Phys. Rev. Lett.* **84**, 4240 (2000).
  - [12] A. L. Lin, A. Hagberg, E. Meron, and H. L. Swinney, Resonance tongues and patterns in periodically forced reaction-diffusion systems, *Phys. Rev. E* **69**, 066217 (2004).
  - [13] D. C. Cole and S. B. Papp, Subharmonic Entrainment of Kerr Breather Solitons, *Phys. Rev. Lett.* **123**, 173904 (2019).
  - [14] J. K. Jang, A. Klenner, X. Ji, Y. Okawachi, M. Lipson, and A. L. Gaeta, Synchronization of coupled optical microresonators, *Nat. Photonics* **12**, 688 (2018).
  - [15] J. K. Jang, X. Ji, C. Joshi, Y. Okawachi, M. Lipson, and A. L. Gaeta, Observation of Arnold Tongues in Coupled Soliton Kerr Frequency Combs, *Phys. Rev. Lett.* **123**, 153901 (2019).
  - [16] J. Hillbrand, D. Auth, M. Piccardo, N. Opačak, E. Gornik, G. Strasser, F. Capasso, S. Breuer, and B. Schwarz, In-Phase and Anti-Phase Synchronization in a Laser Frequency Comb, *Phys. Rev. Lett.* **124**, 023901 (2020).
  - [17] J. Sheng, X. Wei, C. Yang, and H. Wu, Self-Organized Synchronization of Phonon Lasers, *Phys. Rev. Lett.* **124**, 053604 (2020).
  - [18] C. C. Rodrigues, C. M. Kersul, A. G. Primo, M. Lipson, T. P. M. Alegre, and G. S. Wiederhecker, Optomechanical synchronization across multi-octave frequency spans, *Nat. Commun.* **12**, 5625 (2021).
  - [19] M. Lowe, J. P. Gollub, and T. C. Lubensky, Commensurate and Incommensurate Structures in a Nonequilibrium System, *Phys. Rev. Lett.* **51**, 786 (1983).
  - [20] P. Coulet, Commensurate-Incommensurate Transition in Nonequilibrium Systems, *Phys. Rev. Lett.* **56**, 724 (1986).
  - [21] R. Manor, A. Hagberg, and E. Meron, Wave-number locking in spatially forced pattern-forming systems, *Europhys. Lett.* **83**, 10005 (2008).
  - [22] R. Manor, A. Hagberg, and E. Meron, Wavenumber locking and pattern formation in spatially forced systems, *New J. Phys.* **11**, 063016 (2009).
  - [23] D. G. Míguez, M. Dolnik, I. Epstein, and A. P. Munuzuri, Interaction of chemical patterns in coupled layers, *Phys. Rev. E* **84**, 046210 (2011).
  - [24] A. S. Mikhailov and K. Showalter, Control of waves, patterns and turbulence in chemical systems, *Phys. Rep.* **425**, 79 (2006).
  - [25] D. Walgraef, External forcing of spatio-temporal patterns, *Europhys. Lett.* **7**, 485 (1988).
  - [26] I. Rehberg, S. Rasenat, J. Fineberg, M. de la Torre Juárez, and V. Steinberg, Temporal Modulation of Traveling Waves, *Phys. Rev. Lett.* **61**, 2449 (1988).
  - [27] H. Chaté, A. Pikovsky, and O. Rudzick, Forcing oscillatory media: Phase kinks vs. synchronization, *Phys. D: Nonlinear Phenom.* **131**, 17 (1999).

- [28] S. Rüdiger, D. G. Míguez, A. P. Muñozuri, F. Sagués, and J. Casademunt, Dynamics of Turing Patterns under Spatiotemporal Forcing, *Phys. Rev. Lett.* **90**, 128301 (2003).
- [29] S. Rüdiger, E. Nicola, J. Casademunt, and L. Kramer, Theory of pattern forming systems under traveling-wave forcing, *Phys. Rep.* **447**, 73 (2007).
- [30] A. Beetz, C. Gollwitzer, R. Richter, and I. Rehberg, Response of a ferrofluid to traveling-stripe forcing, *J. Phys.: Condens. Matter* **20**, 204109 (2008).
- [31] A. Rosen, R. Weill, B. Levit, V. Smulakovsky, A. Bekker, and B. Fischer, Experimental Observation of Critical Phenomena in a Laser Light System, *Phys. Rev. Lett.* **105**, 013905 (2010).
- [32] D. Kielpinski and O. Gat, Phase-coherent repetition rate multiplication of a mode-locked laser from 40 MHz to 1 GHz by injection locking, *Opt. Express* **20**, 2717 (2012).
- [33] O. Gat and D. Kielpinski, Frequency comb injection locking of mode locked lasers, *New J. Phys.* **15**, 033040 (2013).
- [34] V. I. Arnold, *Geometrical Methods in the Theory of Ordinary Differential Equations*, 2nd ed., Grundlehren der mathematischen Wissenschaften, Vol. 250 (Springer, New York, 1988).
- [35] J. M. Soto-Crespo, Stability of the pulselike solutions of the quintic complex Ginzburg-Landau equation, *J. Opt. Soc. Am. B* **13**, 1439 (1996).
- [36] V. I. Arnold, Small denominators. I. Mapping the circle onto itself, *Izv. Akad. Nauk SSSR Ser. Mat.* **25**, 152 (1961).